Chemical Engineering Journal 425 (2021) 130498

Contents lists available at ScienceDirect

Chemical Engineering Journal

journal homepage: www.elsevier.com/locate/cej

Nano-in-Nano dendrimer gel particles for efficient topical delivery of antiglaucoma drugs into the eye

Juan Wang [a], Boxuan Li [b], Da Huang [c], Pedro Norat [d], Marta Grannonico [d], Remy C. Cooper [e], Qin Gui [f], Woon Nam Chow [g,h], Xiaorong Liu [d,i,*], Hu Yang [c,*]

[a] College of Biomedical Engineering, Sichuan University, Chengdu, Sichuan 610065, China
[b] Tianjin Key Laboratory of Biomedical Materials, Key Laboratory of Biomaterials and Nanotechnology for Cancer Immunotherapy, Institute of Biomedical Engineering, Chinese Academy of Medical Sciences & Peking Union Medical College, Tianjin 300192, China
[c] Linda and Bipin Doshi Department of Chemical and Biochemical Engineering, Missouri University of Science and Technology, Rolla, MO 65409, United States
[d] Department of Biology, University of Virginia, Charlottesville, VA 22904, United States
[e] Department of Biomedical Engineering, Virginia Commonwealth University, Richmond, VA 23298, United States
[f] Department of Chemical and Life Science Engineering, Virginia Commonwealth University, Richmond, VA 23219, United States
[g] Department of Pathology, Virginia Commonwealth University, Richmond, VA 23298, United States
[h] Department of Ophthalmology, Virginia Commonwealth University, Richmond, VA 23298, United States
[i] Department of Psychology, University of Virginia, Charlottesville, VA 22904, United States

ARTICLE INFO

Keywords:
Dendrimer
Microgel
Nanogel
Brimonidine
Glaucoma

ABSTRACT

Low bioavailability of topically applied drugs remains a significant challenge for long-term glaucoma therapy. To enhance drug delivery efficiency, we developed dendrimer gel particles that collectively exhibit structural benefits of dendrimer, hydrogel, and particles, using the inverse emulsion method coupled with the highly efficient aza-Michael addition reaction (IEaMA). This hierarchical approach would maximize the utility of the structural features of existing ocular drug delivery systems. We have tested the delivery efficiency and efficacy of two first-line antiglaucoma drugs, brimonidine tartrate (BT) and timolol maleate (TM), which were loaded into dendrimer gel particles of various sizes, i.e., nDHP (nano-in-nano dendrimer hydrogel particles, ~200 nm), μDHP3 (3 μm), and μDHP10 (9 μm). We found that nDHP was superior to μDHP3 and μDHP10 in terms of cytocompatibility, degradability, drug release kinetics, and corneal permeability. The nDHPs increased drug corneal permeability by 17-fold compared to plain drug solution and enabled zero-order prolonged drug release kinetics. The nDHP-based formulation demonstrated pronounced IOP-lowering effects in both single-dose test and 7-day chronic daily dosing test in both Brown Norway rats and glaucoma mice. Taken together, we have developed nano-in-nano dendrimer gel particles for precise dosing and enabling sustained and synergistic efficacy of antiglaucoma drugs, which could be clinically impactful for improving glaucoma treatment.

1. Introduction

Glaucoma remains a leading cause of blindness worldwide. The number of glaucoma patients will rise to 111.8 million in 2040 [1]. Elevated intraocular pressure (IOP) is a characteristic risk factor of glaucoma. All current treatments are to lower or control IOP and thereby slow down or reduce the subsequent vision loss [2]. Treatment typically begins with topical antiglaucoma medications. Topically administered drugs, however, have bioavailability of<5% due to high pre-corneal loss and low cornea permeation [3–6]. Frequent daily dosing of ocular hypotensive medication further raises the concerns of delivery effectiveness and patient adherence to the therapy, a major obstacle for successful glaucoma management [7–10].

Using particles ranging in size from nanometers to microns to improve bioavailability and sustain the efficacy of antiglaucoma drugs is on the horizon [11–17], but there are two main challenges. First, size, structure, and physicochemical properties of particles, such as surface charges, composition, and mucin adhesiveness [18], are essential to tune particles to overcome ocular barriers to gain enhanced preocular retention, corneal permeation, and absorption. The challenge is how to

* Corresponding authors at: Linda and Bipin Doshi Department of Chemical and Biochemical Engineering, Missouri University of Science and Technology, Rolla, Missouri 65409, United States.
E-mail addresses: xl8n@virginia.edu (X. Liu), huyang@mst.edu (H. Yang).

https://doi.org/10.1016/j.cej.2021.130498
Received 2 February 2021; Received in revised form 18 May 2021; Accepted 21 May 2021
Available online 28 May 2021

build a particulate system that synchronizes particle transport to the anterior chamber of the eye with drug delivery and release kinetics. Secondly, when first-line monotherapy for glaucoma becomes ineffective, two or three drugs are often combined to produce additional IOP reduction. Those drugs in the free drug form in ophthalmic solution are unlikely to reach the eye at the ratio prescribed due to the variance in physicochemical properties and corneal permeation, bringing about only suboptimal therapeutic outcomes. Features such as high loading capacity and versatility that enables accommodating drugs of distinct pharmacological and physicochemical properties are thus desired.

We attempted to address the above two issues by using polyamidoamine (PAMAM) dendrimers as building blocks [19,20]. PAMAM dendrimers are highly branched nanostructured synthetic polymers [21], ideal for drug and gene delivery, primarily due to their multivalency, enabling multi-functionalization and electrostatic interactions [22]. Furthermore, PAMAM dendrimers exhibit unimolecular micelle encapsulation behavior [23]. Hydrophobic drugs can be encapsulated into dendrimer interior cavities via host–guest interactions. However, such host–guest interactions may be disrupted easily under physiological conditions, causing premature drug leakage and uncontrolled release, a major limitation for dendrimer-based drug encapsulation and delivery.

To expand the capacity of dendrimers for drug encapsulation and delivery, we developed a new method, i.e., the inverse emulsion aza-Michael addition reaction (IEaMA) method, to make dendrimer hydrogel particles (DHPs) [24]. DHPs integrate the advantages of dendrimer, hydrogel and nano/micro-particle. Therefore, DHPs hold great promise to be used to deliver multiple antiglaucoma drugs for development of the next generation of dendrimer-based antiglaucoma drug delivery systems. DHPs are highly swellable in physiological solution and appear as transparent colloidal dispersions, eliminating themselves as a source for blurred vision or eye irritation [25]. In this work, we demonstrated that DHPs in the nanometer to micrometer range can be made by tuning parameters of the IEaMA-based process: oil-to-water ratio, surfactant concentration, and stirring speed. The two first-line IOP-lowering drugs, brimonidine tartrate (BT) and timolol maleate (TM), were used as model drugs and packaged into DHPs. The delivery efficiency and safety of DHPs with three discrete sizes, i.e., nano-in-nano DHP (nDHP) on a scale of hundreds nanometers (~200 nm) and two micronized DHPs—μDHP3 (3 μm), and μDHP10 (9 μm)—were assessed. We found that nDHP was superior to μDHP3 and μDHP10 in terms of cytocompatibility, degradability, drug release kinetics, and corneal permeability. In vivo tests using both normotensive rats and glaucoma mice showed that nDHP-based formulation induced more pronounced IOP-lowering effects in both single-dose test and 7-day once-daily dosing test.

2. Materials and methods

2.1. Materials

DAB-core PAMAM dendrimer generation 5 (G5) was purchased from NanoSynthons (Mt Pleasant, MI). Poly(ethylene glycol) diacrylate (PEG-DA, M_n = 575 g/mol), span80, tween80, fluorescein isothiocyanate isomer I (FITC), trifluoroacetic acid (TFA), and cell proliferation reagent WST-1 were purchased from Sigma-Aldrich (St. Louis, MO). Brimonidine tartrate (BT) was purchased from AvaChem Scientific (San Antonio, TX). Timolol maleate (TM), hexane, acetonitrile (ACN), and phosphate buffered saline (PBS, 10×) were purchased from Fisher Scientific (Pittsburgh, PA). Triton X-100 was purchased from Solarbio Life Sciences (BJ, CN). Dulbecco's modified Eagle's medium (DMEM), trypsin-EDTA (0.25%), and penicillin–streptomycin (10,000 U/mL) were purchased from Life Technologies (Carlsbad, CA). ELISA kits of human TNF-α and IL6 were purchased from Thermo Fisher Scientific (Waltham, MA). Contrived tears developed from greater than 15 components known to be present in tears, balancing protein, salt and pH alike, in line with accepted tear formulations, was purchased from Ursa BioScience (Maryland, USA). Fresh rabbit whole eyes were purchased from Pel-Freeze Biologicals (Rogers, AR). Cell culture medium for primary human corneal epithelial cells (HCECs) was purchased from American Type Culture Collection (ATCC, Manassas, VA).

2.2. Characterization

A field emission SEM microscope (Hitachi FE-SEM Su-70, Japan) with an acceleration voltage of 5 kV was used to image μDHPs, and JEM-1400 Plus TEM for nDHPs. The hydrodynamic sizes and zeta potentials of DHPs were measured on Zetasizer Nano-ZS90 (Malvern Instruments, U.K.). Antiglaucoma drug released from DHPs was quantified by using a Waters HPLC system equipped with a dual absorbance UV detector. The mobile phase was the mixture of acetonitrile, water, and trifluoroacetic acid (1/1/0.05 v/v/v). Eluents were monitored at both 309 and 220 nm.

2.3. Preparation of DHPs

DHPs were prepared by using the IEaMA method developed by us [24]. The oil phase was a mixture of hexane and surfactant (Table S1). The aqueous solution was prepared by mixing G5 (10 wt%) and PEG-DA (the molar ratio of amine/acrylate = 1/1) in deionized water followed by vortex for 10 s. The oil-to-water volume ratio (O/W) was tuned to obtain different micro-nano particle sizes (Table S1). For μDHP preparation, the aqueous solution was poured into the oil phase and dispersed at 30,000 rpm for 60 s by using an IKA disperser. The emulsion system was then stirred at 500 rpm for 2 h, allowing the cross-linking within the stabilized emulsion droplets to form DHPs. For nDHP preparation, the aqueous solution was added to the oil phase and directly stirred at 500 rpm for 2 h by using an IKA stirrer. The mixture was then centrifuged (4,900 rpm for μDHPs and 10,000 rpm for nDHPs) for 3 min, and the oil layer was discarded. The residue was washed with deionized water 3 times to obtain surfactant-free DHPs.

To prepare drug-loaded μDHPs and nDHPs, drugs were mixed with G5 aqueous solution (10 wt%) prior to mixing with PEG-DA. Specifically, 1 mg of BT or TM was added to 53 μL of 10 wt% of G5 aqueous solution, followed by vortex and sonication to make a clear solution. Drug loading was measured by HPLC. On the basis of 1 mg particle, μDHP10 carries 272.2 μg of BT, μDHP3 carries 215.1 μg of BT, and nDHP contains 8.6 μg of BT.

2.4. Degradation studies

DHPs in dry form (w_0) were dispersed in contrived tears (0.5 mL) and incubated at 37 ℃ for 6 h, 24 h, and 48 h, respectively. At the end of incubation, dispersions were subjected to centrifugation (10,000 rpm, 3 min). The pellet was washed once with deionized water and then freeze-dried and weighed (w_t). Mass remaining (%) was determined as $w_t/w_0 \times 100$. The degraded μDHPs were imaged by using SEM [24].

2.5. Drug release studies

In general, BT-loaded DHPs were dispersed in 1 mL of pH 7.4 PBS and kept at 37 ℃. At predetermined time points, the suspension was subjected to centrifugation (10,000 rpm, 3 min). The supernatant was collected for BT concentration analysis. The pellet was re-suspended in 1 mL of fresh PBS to continue the release study. Each formulation was tested three times under identical conditions. Cumulative BT release as a function of time was reported and release kinetics models were used to study release mechanisms [26].

2.6. Ex vivo permeation studies

Cornea extracted from fresh rabbit eye was mounted in a Franz diffusion cell system [27]. The receiver chamber was filled with 5 mL of pH 7.4 PBS. BT-loaded DHPs suspended in 250 μL of PBS was loaded to the donor chamber. At pre-determined time points up to 4 h, an aliquot

of 500 μL was withdrawn from the receiver chamber and analyzed with HPLC. Fresh PBS (500 μL) was added to the receiver chamber following each sampling. The permeability coefficient, *P*, was then determined [28]. Each experiment was repeated three times.

2.7. Cytotoxicity assessment

NIH3T3 fibroblast cells or HCECs were seeded at a density of 1×10^4 cells/well in a 96-well plate and cultured overnight. The ATCC medium for HCEC supplemented with Corneal Epithelial Cell Growth Kit components (apo-transferrin, epinephrine, extract P, hydrocortisone hemisuccinate, L-glutamine, rh insulin, and CE growth factor) was prepared following the manufacturer's instructions. The cells were then incubated with DHPs at various concentrations (0–1.25 mg/mL) for 48 h. DHPs were freshly prepared, lyophilized followed by ultraviolet sterilization for 0.5 h and then dispersed in sterile PBS before incubation. Given that (1) filtration sterilization is recommended for future clinical usage and (2) nDHP is highly squeezable and its hydrodynamic diameter is 209 nm, filtration through 0.2-μm pore size is another possible sterilization method. Cell viability relative to untreated cells was then determined by using the WST-1 proliferation assay [29]. The IC50 of nDHP on HCEC was calculated following a four-parameter logistic regression (4PL) fitting.

Pro-inflammatory cytokines TNF-α and IL6 released from HCECs were quantified. Briefly, HCECs were seeded in 24-well plate (1×10^5 cells/well) and cultured 24 h. The medium of each well was replaced with fresh medium containing nDHP at different concentrations (50, 87.5, or 125 μg/mL). Following 4 h incubation, the culture media were collected and centrifuged. The supernatants were subjected to ELISA analysis following the manufacturer's instructions.

2.8. Hemolysis toxicity

Hemolysis assay was performed to evaluate the membrane damaging effect of DHPs. Whole rabbit red blood (2 mL) were centrifuged at 3500 rpm for 10 min. The top two layers (plasma, leukocytes, and platelets) were discarded, and the pellet (erythrocytes) was collected and washed with sterile PBS (pH 7.4) to ensure no cell lysis. Erythrocytes were then re-suspended with 10 mL of sterile PBS (pH 7.4). To 750 μL of erythrocyte suspension, 50 μL of μDHP10, μDHP3, nDHP, G5, PEG-DA (0.5% w/v), PBS (negative control) and Triton X-100 (1% w/v, positive control) were added respectively and incubated for 1 h, 2 h, and 3 h under mild shaking at 37 ℃. For μDHP10, μDHP3, nDHP, and G5, a concentration of 0.5% w/v G5 equivalent was used. At pre-determined timepoints, samples were centrifuged and 100 μL of supernatant was withdrawn. The absorbance of each supernatant sample was read by using a microplate reader (VERSAmax, Molecular Devices) at 450 nm wavelength. Hemolysis percentage was then calculated using the equation below [30].

$$\text{Hemolysis}(\%) = \frac{\text{Absorbance of sample} - \text{Absorbance of PBS}}{(\text{Absorbance of TritonX} - 100) - \text{Absorbance of PBS}}$$

2.9. In vivo IOP measurements in normotensive glaucoma model

Normotensive adult Brown Norway female rats (Charles River, Wilmington, MA), 5 months old, were used and housed under proper conditions at Virginia Commonwealth University (VCU). The rats were kept under a cycle of 12-h light and 12-h dark. The animal protocol AD10001426 was approved by the institutional animal care and use committees of VCU.

2.9.1. Single-dose assessment

Eight rats were randomly divided into two groups (n = 4), and they received topical treatment of BT/PBS or BT/nDHP (2 × 5 μL, 0.1% w/v BT equivalent). nDHPs for in vivo studies are freshly prepared, lyophilized followed by ultraviolet sterilization for 0.5 h and then dispersed in sterile PBS before administrated. The right eye of each rat was dosed while the left eye was left untreated. The IOPs of both eyes were measured immediately before treatment (0 h) and at 0.75, 1.6, 4.25, and 24 h postdosing using ICare TONOLAB tonometer.

2.9.2. One week of daily dosing assessment

Ten rats were randomly grouped to two (n = 5) and their right eyes received BT/PBS or BT/nDHP^{FITC} (2 × 5 μL, 0.1% w/v BT equivalent) topically at 8:00 am each day for 7 days. The IOPs of both the right eye and the left eye were measured immediately before and after administration and 4 h later. At the end of experiment, rats were euthanized, and eyeballs were removed and processed to obtain tissue slices and H&E stained slices. Tissue images were taken under Nikon inverted microscope ECLIPSE Ti-U and analyzed using ImageJ.

2.10. In vivo IOP evaluation in a genetic glaucoma model

Angiopoietin 1 gene knockout mice (A1 cKO mice, seven months old, n = 4) with elevated IOP were used as a glaucoma disease model [31]. In each group, the right eyes were topically treated with BT/nDHP (4 μL, 0.15% w/v BT equivalent) and TM/nDHP (4 μL, 0.5% w/v TM equivalent), while the left eyes were treated with a control solution composed of free non-formulated drugs (BT and TM) at the same dose. The IOP was monitored at pre-determined time intervals. The animal protocol 4173 was approved by the institutional animal care and use committees of University of Virginia.

2.11. Statistical analysis

The data were expressed as means ± standard deviation (SD) and were analyzed using one-way analysis of variance (ANOVA). A value of $p < 0.05$ was considered statistically significant. The adjusted means of IOP reduction (△IOP) at 12 PM each day following one week of daily dosing on rats is derived using an analysis of covariance adjusted for baseline IOP and based on observed data for all randomized subjects.

3. Results

3.1. Size-tunable dendrimer gel particles

The inverse emulsion method was adopted for producing the micro/nanodroplets (Scheme 1). Multiple parameters such as surfactant composition (tween80/span80 ratio), surfactant-to-hexane ratio, O/W ratio, and dispersion intensity were used to manipulate gel particle size (Table S1). We prepared dendrimer gel particles smaller than 10 μm as larger particles tend to induce foreign body sensation and reflex tearing [6]. μDHP10 (Fig. 1a) and μDHP3 (Fig. 1b) are spherical. SEM image analysis revealed that their mean diameters are 8.7 ± 0.2 μm and 3.3 ± 0.4 μm, respectively. This method also generates uniform nanogels (78 ± 19 nm) (Fig. 1c). Dendrimer micro/nanogels are micro/nanosized swellable networks in solution and the gel particles can be dispersed into PBS to form colloidal suspension. The swollen dendrimer gel particles experienced significant size expansion. In particular, the diameter of μDHP3 increased to 4.0 μm (PDI = 0.299), and nDHP has a diameter of 209.6 nm (PDI = 0.284) (Fig. 1d). The hydrodynamic size of swollen μDHP10 exceeded the detection limit (10 μm diameter) of the DLS instrument. Our SEM/TEM images and DLS results showed the typical micro/nanogel structures, morphologies and size features, consistent with the characterization of micro/nanogels reported in literatures. The positively charged surfaces of all the three particles were confirmed by their ζ potential values of 29.0 ± 3.1 mV, 22.1 ± 2.0 mV, and 12.9 ± 0.3 mV for μDHP10, μDHP3, and nDHP, respectively, which are significantly different with the ζ potential value of unmodified G5 (50.4 ± 0.1 mV, the *P* values of μDHP10, μDHP3, nDHP *vs* G5 are 1.3×10^{-4}, 7.5×10^{-6}, 2.2×10^{-9}, respectively, Fig. 1e).

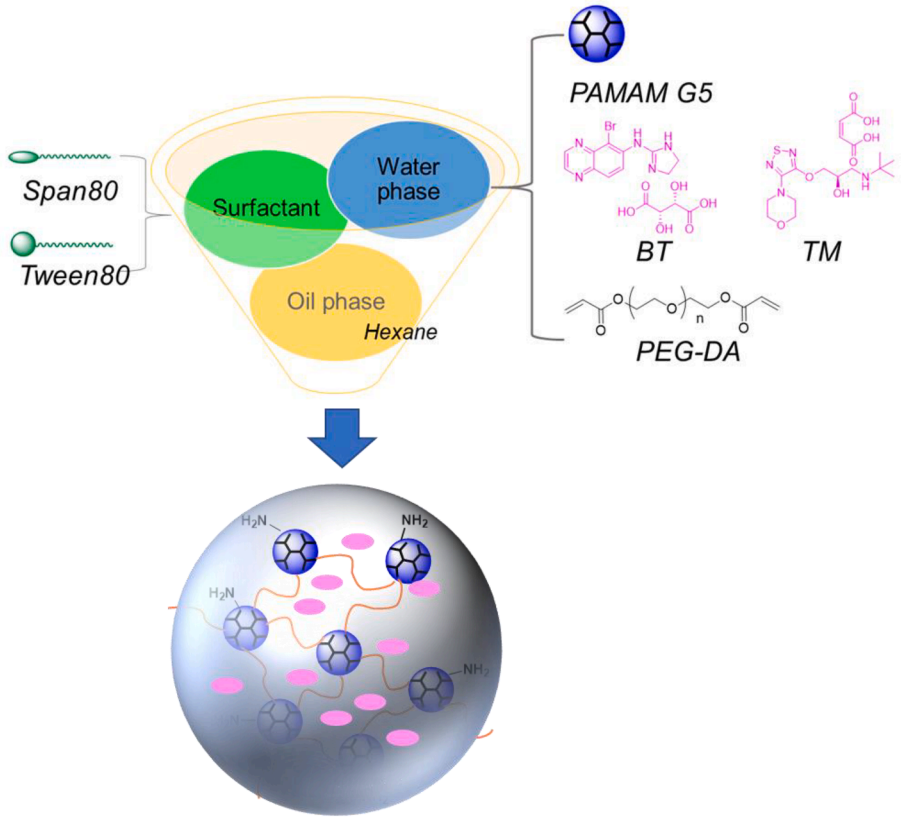

Scheme 1. Schematic illustration of the preparation of dendrimer gel particles of various sizes by using the invert emulsion method coupled with aza-Michael addition reaction and tuning three parameters oil-to-water ratio, surfactant concentration, and stirring speed.

3.2. *In vitro degradation and safety assessment*

The prepared dendrimer gel particles (μDHP10, μDHP3, and nDHP) were further assessed in terms of cytotoxicity, degradability, drug release and corneal permeability. nDHP maintains much higher cytocompatibility than μDHP10 and μDHP3. When particle concentration is at or lower than 50 μg/mL (equivalent to 20 μg/mL of G5), none of them cause apparent cytotoxicity to NIH3T3 cells (Fig. 2a). As the concentration increases to 1.25 mg/mL (equivalent to 500 μg/mL of G5), μDHP10 and μDHP3 cause 33% of cell death, 2.8-fold higher than cell death induced by nDHP.

We studied the in vitro degradation kinetics of dendrimer gel particles incubated in contrived tears. During the first 6 h-incubation, μDHP10, μDHP3, and nDHP were relatively stable and experienced negligible mass loss (Fig. 2b). When incubation was extended to 24 h, more than 70% of μDHP10 degraded. <17% of μDHP10 remained after 48-h incubation. μDHP3 degraded more slowly. Approximately 19% of its mass remained after 48-h incubation. Moreover, more than 40% of nDHPs remained intact at 48 h post-incubation. μDHP10 and μDHP3 maintained their particle morphology but became porous and flattened over the observation period of 48 h (Fig. S1). The hemolytic toxicity of DHPs was assessed along with G5 and PEG-DA. As shown in Fig. S2, none of the tested groups has shown substantial hemolytic behavior, indicating their good blood compatibility.

3.3. *nDHP enables zero-order drug release kinetics and superb corneal permeability*

The release of BT from μDHP10 and μDHP3 was quick. Nearly 100% of the encapsulated BT molecules were released within 2 h via Fickian diffusion (Fig. 2c). Within the first 6 h, 74% of BT was released from nDHP. Furthermore, BT release from nDHP followed zero-order release kinetics, a release mechanism that could control antiglaucoma drug release for sustained efficacy.

nDHP brings more BT across the cornea. Within 2 h, nDHP enabled 4.1 μg of BT to permeate through the cornea while μDHP10, μDHP3 resulted in cumulative amounts of 2.4 μg and 3.5 μg of BT across the cornea. Furthermore, permeability coefficients for BT mediated by μDHP10, μDHP3, and nDHP are 3.5×10^{-7} cm/s, 1.5×10^{-6} cm/s, and 7.6×10^{-6} cm/s, respectively (Fig. 2d).

The permeability was further tested by using FITC-labeled microgel and DiR-labeled microgel, respectively. As shown in Fig. S3a, no FITC was detected permeated across the cornea in the first 2 h. At 4 h, there are 62% of FITC crossed the cornea. The DiR signals (Fig. S3b) in the eye indicate gel particles permeated through the cornea and transported in Schlemm's canal.

3.4. *nDHP sustains in vivo IOP lowering effects*

The IC50 of nDHP on HCEC is 0.42 mg/mL. A dose of 0.25 mg/mL of nDHP or lower is deemed safe (Fig. 3a). We assessed the production levels of proinflammatory cytokines, TNF-α and IL6 in HCECs in response to different doses of nDHPs (Fig. 3b). Unmodified PAMAM dendrimers show proinflammatory activities in vivo [32]. It is reported that 0.8 μM of G5 could induce 200 pg/mL of TNF-α secretion, and 400 pg/mL of IL6 secretion in J774A.1 macrophage cells [33]. At the tested doses, nDHPs did not stimulate TNF-α production. nDHP at doses as high as 125 μg/mL (equivalent to 3.5 μM of G5) caused 279 pg/mL of IL6 production, 35% higher compared to the baseline (the *P* values of μDHP10, μDHP3, nDHP *vs* Untreated are 0.0022, 0.0022, 0.0019, respectively). The TNF-α and IL-6 levels are 90% and 15% higher in patients receiving preserved latanoprost than in normal controls [34].

The IOP-lowering effect of a single dose of BT/nDHP was examined in normotensive rats and compared with the BT/PBS control group. Both

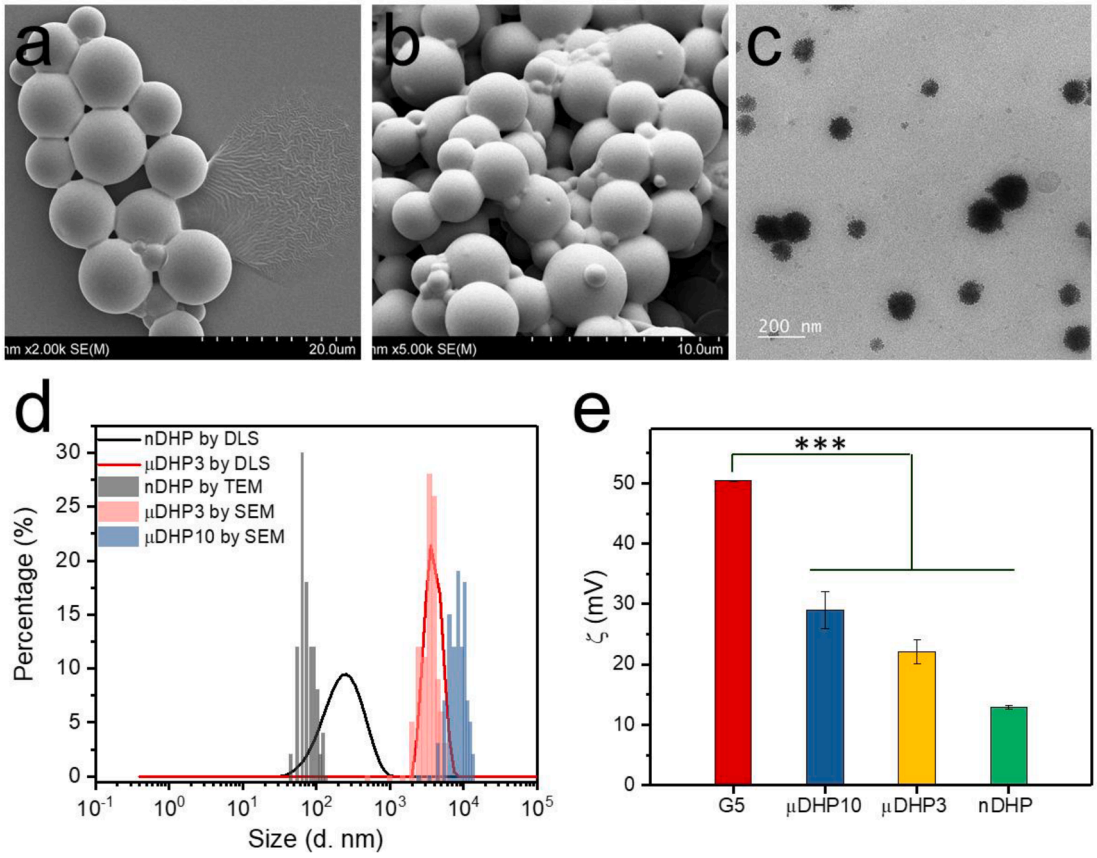

Fig. 1. Morphology, size and zeta potential characterizations of micro/nano dendrimer hydrogel particles. a) SEM image of μDHP10, b) SEM image of μDHP3, c) TEM image of nDHP, d) size distributions, and e) zeta potentials, *** $P < 0.001$ vs G5.

formulations started to reduce IOP immediately after administration and exhibited peak effects at approximately 4 h. But BT/nDHP causes an average of 4.5 mmHg IOP reduction, 2.6-fold stronger than the IOP reduction by BT/PBS eye drops ($P = 0.011$, Fig. S4). The IOP-lowering effects of both formulations diminished afterward over the course of 24 h. Once-daily dosing of BT/nDHP resulted in cumulative IOP-lowering effects (Fig. 4). BT/nDHP exhibits a sustained prominent IOP-lowering effect following 7-day once-daily dosing regimen. The IOP lowering efficacy treated by BT/nDHP at day 7 was 4-fold higher than that treated by BT/PBS ($P = 0.014$, Fig. 4a). According to the covariance analysis that was performed to eliminate the effect of initial IOP (baseline) on IOP reduction, the adjusted means of IOP reduction following BT/nDHP treatment are higher than that of BT/PBS every day (Fig. 4b), over 6-fold higher potency than BT/PBS in terms of IOP reduction on day 1-3. Sustained retention of FITC-labeled nDHP in the cornea was confirmed at the end of treatment (Fig. S5). BT/nDHP does not cause any irritation, including abnormal tearing and blinking (Fig. 5a). Whole-mount histologic globe preparations show that BT/nDHP does not cause any discernable architectural or pathologic changes to ocular tissue elements (Fig. 5b). Furthermore, the structural integrity of the various intraocular compartments, including the anterior and posterior chambers, remains intact (Fig. 5c).

The IOP-lowering effects of nDHP-based antiglaucoma fixed combination therapy, i.e., BT/nDHP&TM/nDHP, were examined in Angiopoietin 1 gene knockout (A1 cKO) mice, a genetic model of open-angle glaucoma. Before drug application, both eyes of A1 cKO mice had an average of IOP of (23 ± 3) mmHg, significantly higher than the wild type baseline IOP, which was around 15 mmHg (Fig. 6a) [31]. The IOP elevation was stable, and it showed no fluctuation daily either (Fig. 6a). Both eyes of A1 cKO mice received a dose of fixed combination topically, with one eye treated with free drugs and the other eye with formulated drugs. IOP reduction is observed in both eyes treated with free drugs and formulated drugs at 1 h and 24 h post-treatment (n = 6). The nDHP treated groups exhibited an IOP value of 19.65 ± 1.94 mmHg at 1 h post treatment, which was significantly lower than that of the free group (22.28 ± 0.96 mmHg), with a P value of 0.026. The IOP lowering effect at 24 h of the formulated group (18.68 ± 1.35 mmHg) was also significant than the free drug group (21.15 ± 2.10 mmHg, $P = 0.047$, Fig. 6b). Together, the formulated drug exhibits potent and long-lasting effects on controlling IOP.

4. Discussion

For a macroemulsion, an emulsion usually having micron-sized droplets, high energy input is required [35,36]. The energy input is generally from mechanical devices, including disperser, homogenizer, and ultrasound generator [35]. We prepared μDHPs by using high-shearing dispersion (30,000 rpm) generated by IKA disperser (T10 basic ULTRA-TURRAX). We continued our previous formula of tween80/span80 1/5 (w/w) and surfactant-to-hexane 1/70 (v/v) [24], but only adjusted the O/W ratio from 35/1 (v/v) to 10/1 (v/v) to finally get microgels with different sizes: 3 μm and 9 μm on average. Unlike the macroemulsion, a nanoemulsion with size ranges from 20 to 200 nm could form spontaneously and does not require energy input [36]. Since tween80 has a higher HLB value (Hydrophile-Lipophile Balance) of 15.0 than that of span80 (4.3), an increase of tween80 component helps obtain smaller droplets in this water-in-oil emulsion system. Conditions of tween80/span80 4.5/5 (w/w) and a mild stirring (500 rpm by magnetic stirrer) are used for nanogel formation. A much higher proportion of surfactant with 3.7/70 (v/v) of surfactant-to-hexane is used for nanogel. The O/W ratio to form a nanogel is increased dramatically to 762/1 (v/v).

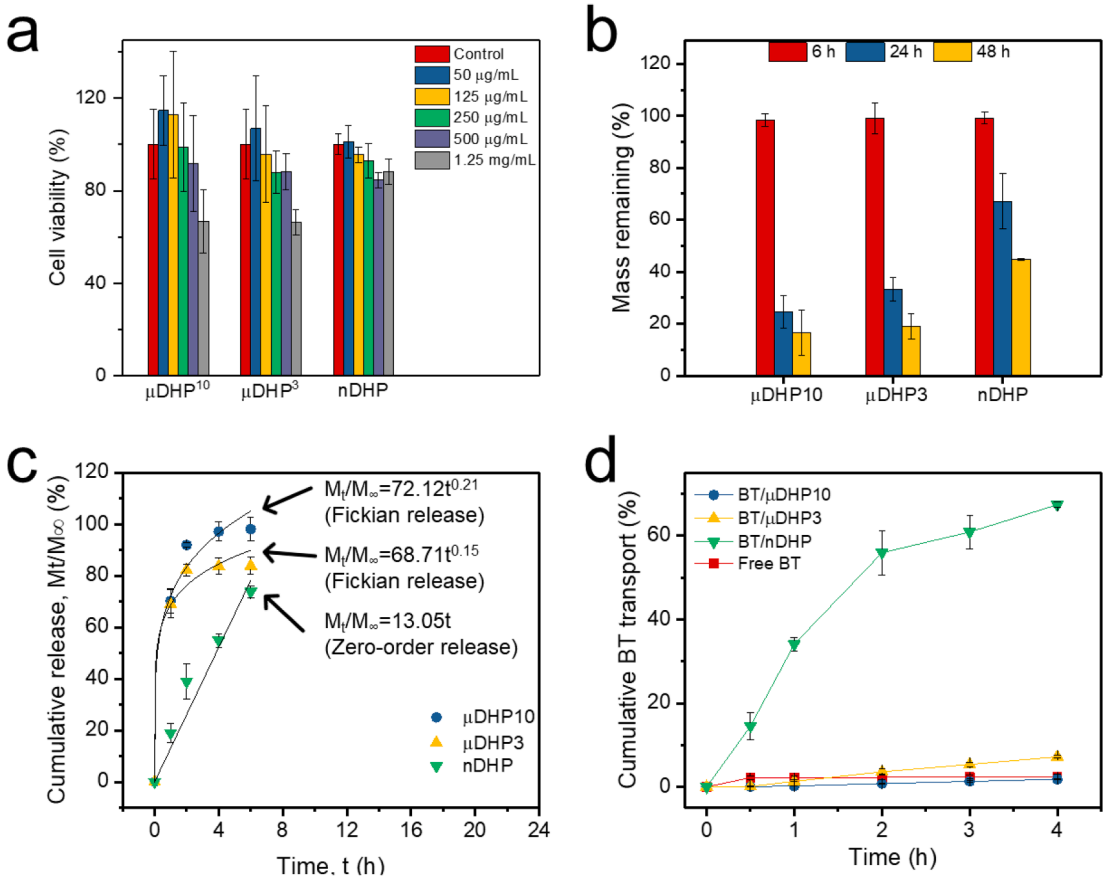

Fig. 2. Assessment on dendrimer micro/nano gel particles. a) Cytotoxicity on NIH3T3 cells following 48-h incubation, n = 8. b) Degradation in contrived tears incubated at 37 ℃, n = 3. c) Drug release, n = 3. d) BT permeation across the cornea, n = 3.

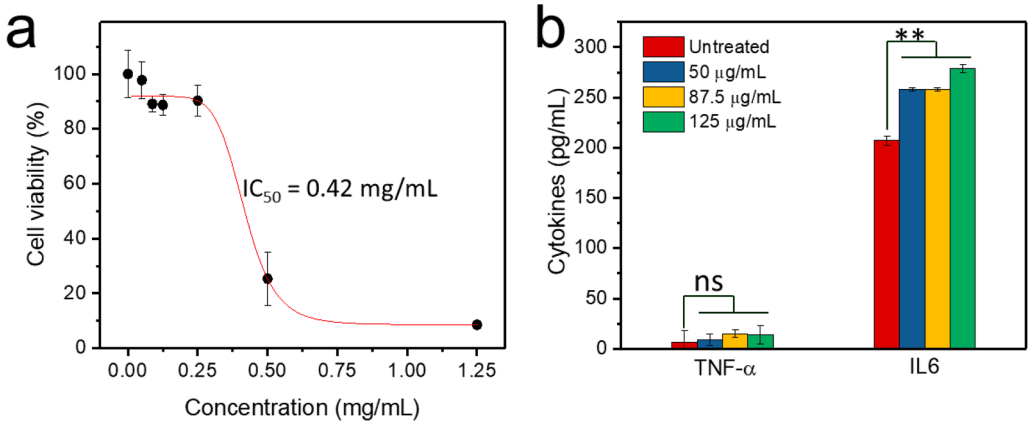

Fig. 3. a) Dose-dependent cytotoxicity of nDHP to HCEC cells after 48 h incubation, n = 8. b) Cytokines of TNF-α and IL6 expression on HCEC after 4 h incubation, n = 4, ** $P < 0.01$ vs Untreated.

The cross-linking reaction of G5 with PEG-DA consumes most, but not all, of the surface amines, resulting in the reduction of surface charges of the formed gel particles. The cross-linking reaction of G5 with PEG-DA is different with PEGylation of dendrimer. PEGylation of dendrimer leads to a modified dendrimer molecule but still a single molecule. However, the formation of dendrimer hydrogel particle is not a simple process of "PEGylation of dendrimers", but rather a process to build a cross-linked structure. The 1:1 amine-to-acrylate ratio and the steric hindrance when a dendritic molecule reacts with a linear polymer chain lead to the generation of a cross-linked network with some amines remaining unreacted. What is interesting is that, under the same reactant concentration (10 wt% of G5), the degrees of un-reacted amines in the gel particles of different sizes vary. Our work suggests that cross-linked dendrimer network on the basis of aza-Michael addition reaction degrade via self-triggered aminolysis, in which unreacted amine groups attack ester bonds in the network [37]. When more amines participate in the cross-linking reaction, the formed network will become more structurally stable because of reduced aminolysis. The degradation kinetics of μDHPs and nDHPs was found to be size-dependent. The smaller the particle size is, the more stable dendrimer gel particles are. nDHP is more stable than μDHP10 and μDHP3. The lack of hemolysis toxicity of DHPs as well as G5 and PEG-DA indicates the blood compatibility of

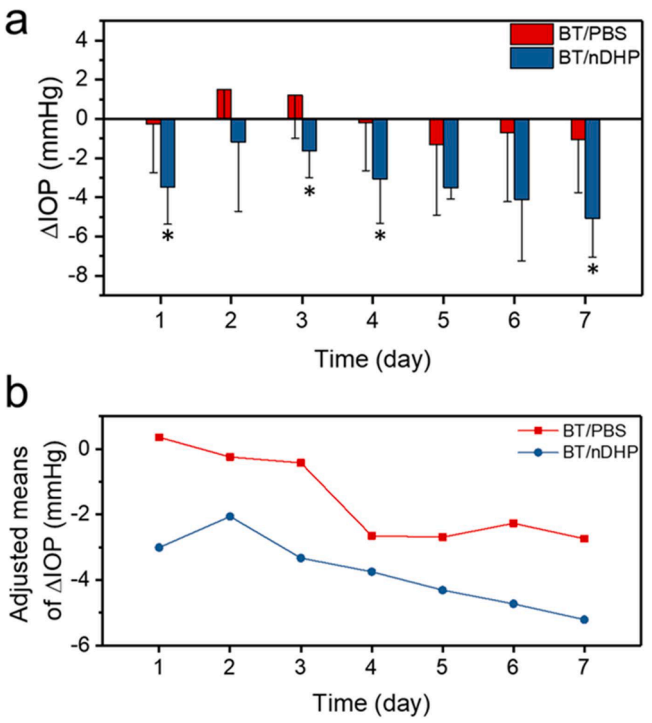

Fig. 4. a) In vivo IOP-lowering effect of BT/nDHP and BT/PBS in normotensive rats after 7- day daily dosing topical administration. * $P < 0.05$ BT/nDHP vs BT/PBS. b) The adjusted means of △IOP at 12 PM each day is derived using an analysis of covariance adjusted for baseline IOP and based on observed data for all randomized subjects. The dose of each formulation is 2 × 5 μL, 0.1% w/v BT equivalent for 7 days.

DHPs.

Although the BT to G5 feed ratio is the same in the water phase, the washing process results in different drug loss and finally leads to different drug loading efficiency for different particles. Compared to the quick release of BT from μDHPs, BT release was extended by nDHP and showed zero-order release kinetics. By comparing the permeability coefficient of free BT, i.e., 4.5×10^{-7} cm/s, μDHP10 does not improve the corneal permeability of BT at all, and μDHP3 only slightly improves BT's corneal permeability. BT from nDHP has obtained the highest permeability coefficient. In addition, for BT/nDHP formulation, the transport of BT across the cornea almost matches its drug release kinetics. It is meaningful for a topical ocular delivery system to synchronize drug transport to the anterior chamber of the eye with drug delivery and release kinetics. The prolonged retention of μDHPs is ascertained by the permeation of FITC-labeled μDHP and the presence of NiR dye-labeled μDHP on the ocular surface. Since there are no cleavable bonds between FITC and dendrimer, and the degradation of microgel particles in 4 h is negligible, it is reasonable to believe that microgel particles have permeated through the cornea. These preliminary studies confirm the μDHP's capacities of both prolonged retention on the cornea and permeation across the cornea.

Since nDHP possesses high cytocompatibility and enables BT to have significantly improved permeability, zero-order release kinetics, we selected nDHP for further in vivo examination. Prior to in vivo studies, we decided a safe dose of nDHP by assessing cytotoxicity of nDHP to human cornea epithelium cells (HCECs), the foremost ocular barrier for topically instilled drugs or formulations. Results show that nDHP is acceptable to be used as topical antiglaucoma drug carrier at appropriate doses. The sustained potent IOP-lowering effect of BT/nDHP from repeat once-daily dosing of BT/nDHP is attributed to the increased corneal permeation, zero-order drug release, and retention in the cornea stroma. This cumulative decline on IOP indicates the nDHP formulation has the great potential to reduce dosing frequency. Angiopoietin/TEK (ANGPT/TEK) signaling is critical for Schlemm's canal (SC) formation and function in mice and humans [31,38]. Mice lacking ANGPT1

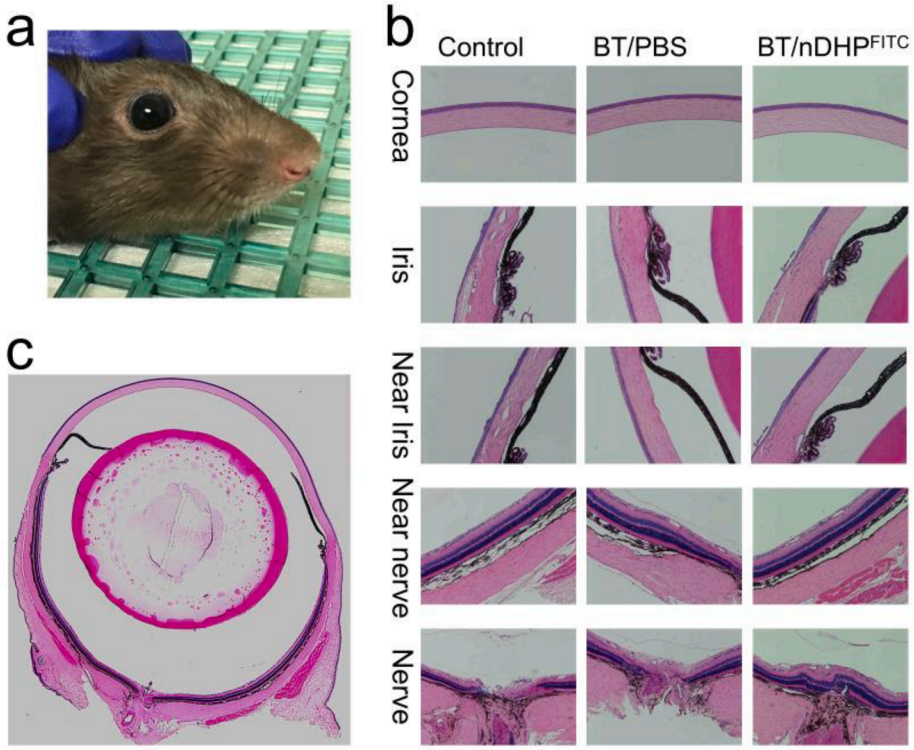

Fig. 5. a) Images of rat eyes immediately after instillation of BT/nDHP^{FITC}. b) Ocular tissues of rat eyes following daily instillation of BT/PBS eye drops and BT/nDHP^{FITC} PBS suspensions for 7 days, magnification 200 × . c) The whole globe tissue images of rat eye after 7 days' instillation with BT/nDHP^{FITC} PBS suspensions.

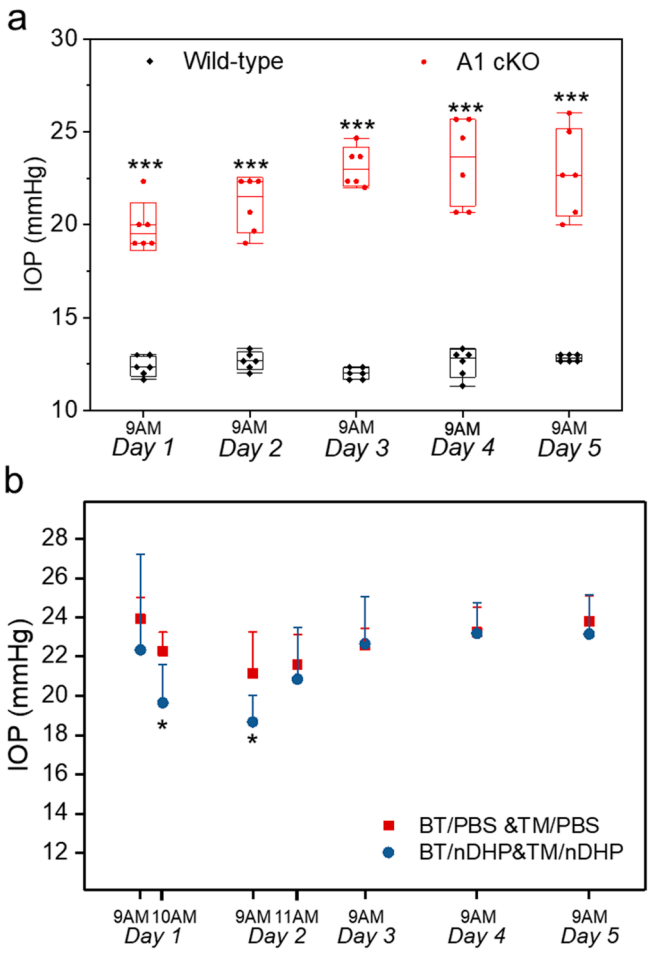

Fig. 6. a) The IOP elevation of A1 cKO mice compared to wildtype littermate controls before formulation treatment. Data present as mean ± SE; n = 6 (left and right eyes of 3 mice); *** $P < 0.001$. b) IOP changes in A1 cKO mice following topical treatment of one dose of BT/PBS&TM/PBS or BT/nDHP&TM/nDHP (4 μL, 0.15% w/v BT equivalent; 4 μL, 0.5% w/v TM equivalent). * $P < 0.05$ vs BT/PBS&TM/PBS.

develop a hypomorphic SC, which is insufficient for normal aqueous humor outflow, resulting in sustained IOP elevation [38–40]. Angiopoietin conditional knockout mice (A1 cKO) exhibit consistent and chronic IOP elevation from about 20-days of age, and the IOP elevation is stable with age for individual mice, which makes it an ideal model system to study the short- and long-term drug effects on IOP regulation. The baseline IOP of wild type mice is around 15 mmHg, and the A1 cKO mice develop ocular hypertension bilaterally, reaching ~ 20 mmHg by 6 weeks of age, and maintain an elevated IOP in adulthood [31]. The reduced IOP in A1 cKO provides further evidence of the delivery efficiency of new formulation. Future studies will be centered on the establishment of the pharmacokinetics of antiglaucoma drugs delivered by nDHP and long-term protection on vision.

In view of the efficient IOP-lowering effect, the flexibility of multi-drug loading and general applicability of this nDHP formulation, a comprehensive mechanistic study including preocular retention, the transport pathway and distribution after topical administration of nDHP will be conducted in future work. The “nano-in-nano” dendrimer gel formulation represents an advanced structure and innovative use of dendrimer building blocks and it holds great potential in the application of glaucoma therapy. The preocular retention study will be carried out using fluorescent dye labeled nDHPs characterized by in vitro immunocytochemistry and in vivo optical coherence tomography (OCT). The pharmacokinetics of antiglaucoma drugs delivered by nDHPs, biodistribution and clearance of nDHPs will also be studied.

5. Conclusions

In this work, we successfully miniaturized dendrimer hydrogel to form nanostructured dendrimer hydrogel particles (nDHPs) using the IEaMA method developed by us. We identified parameters that are essential for fabricating nanostructured dendrimer gel particles. This method enables the scalable production of dendrimer gel particles with tunable size and surface charge, which are closely related to cytocompatibility, corneal permeability, degradation, and drug release. Compared to micron-sized dendrimer gel particles, nDHP promotes corneal permeability and realizes zero-order release kinetics of antiglaucoma drugs. nDHP has a longer residence time in the cornea stroma and makes the encapsulated antiglaucoma drugs exert sustained and stronger IOP-lowering effects as confirmed in normotensive and genetic glaucoma models. Based on its intrinsically new properties and ability to enable antiglaucoma drugs to exert prominent IOP lowering effects, we believe nDHP represents a new generation of advanced platform. Not only do nDHPs retain the DH properties as we demonstrated before, but they also have additional compelling features for antiglaucoma drug delivery as follows: (i) it facilitates corneal permeation of combined drugs at the ratio as prescribed by confining the drugs into particulate structures; (ii) it has high drug encapsulation capacity for both hydrophilic drugs (or drug salt form) and hydrophobic drugs as well as it enables programmable synchronized release of the delivered drugs, a key feature for precise dosing of ocular drugs in combinations; and (iii) nDHPs have the potential for developing more efficient antiglaucoma formulations and deliver emerging classes of new drugs such as Rho kinase inhibitor for therapeutic interventions via multiple mechanisms.

Declaration of Competing Interest

The authors declare that they have no known competing financial interests or personal relationships that could have appeared to influence the work reported in this paper.

Acknowledgments

This work was supported, in part, by the National Institutes of Health (R01EY024072 and R01EY029121) and the Fundamental Research Funds for the Central Universities (Grant No. 20822041D4094, 1082204112665). Services and products in support of the research project were generated by the Virginia Commonwealth University Cancer Mouse Models Core Laboratory, supported, in part, with funding to the Massey Cancer Center from NIH-NCI Cancer Center Support Grant P30 CA016059.

Appendix A. Supplementary data

Supplementary data to this article can be found online at https://doi.org/10.1016/j.cej.2021.130498.

References

[1] Y.-C. Tham, X. Li, T.Y. Wong, H.A. Quigley, T. Aung, C.-Y. Cheng, Global prevalence of glaucoma and projections of glaucoma burden through 2040: a systematic review and meta-analysis, Ophthalmology 121 (2014) 2081–2090, https://doi.org/10.1016/j.ophtha.2014.05.013.
[2] H.A. Quigley, Glaucoma, Lancet 377 (2011) 1367–1377, https://doi.org/10.1016/S0140-6736(10)61423-7.
[3] R.D. Bachu, P. Chowdhury, Z.H.F. Al-Saedi, P.K. Karla, S.H.S. Boddu, Ocular drug delivery barriers—role of nanocarriers in the treatment of anterior segment ocular diseases, Pharmaceutics 10 (2018) 28, https://doi.org/10.3390/pharmaceutics10010028.
[4] C.J.F. Bertens, M. Gijs, F.J.H.M. van den Biggelaar, R.M.M.A. Nuijts, Topical drug delivery devices: a review, Exp. Eye Res. 168 (2018) 149–160, https://doi.org/10.1016/j.exer.2018.01.010.

[5] D. Huang, Y.-S. Chen, I.D. Rupenthal, Overcoming ocular drug delivery barriers through the use of physical forces, Adv. Drug Deliv. Rev. 126 (2018) 96–112, https://doi.org/10.1016/j.addr.2017.09.008.

[6] A. Subrizi, E.M. del Amo, V. Korzhikov-Vlakh, T. Tennikova, M. Ruponen, A. Urtti, Design principles of ocular drug delivery systems: importance of drug payload, release rate, and material properties, Drug Discov. Today 24 (2019) 1446–1457, https://doi.org/10.1016/j.drudis.2019.02.001.

[7] H.A. Quigley, 21st century glaucoma care, Eye 33 (2019) 254–260, https://doi.org/10.1038/s41433-018-0227-8.

[8] L. Golas, C. Marando, L. Seibold, M.B. Pantcheva, P.Y. Ramulu, M.Y. Kahook, J. R. SooHoo, Glaucoma treatments, patient perspectives and preferences, Investig. Ophthalmol. Vis. Sci. 56 (2015) 3703.

[9] V.K. Yellepeddi, S. Palakurthi, Recent advances in topical ocular drug delivery, J. Ocul. Pharmacol. Ther. 32 (2016) 67–82, https://doi.org/10.1089/jop.2015.0047.

[10] L. Dickmann, Ocular therapeutics: drug delivery and pharmacology, Mol. Pharm. 13 (2016) 2875–2876, https://doi.org/10.1021/acs.molpharmaceut.6b00703.

[11] Y. Ikuta, S. Aoyagi, Y. Tanaka, K. Sato, S. Inada, Y. Koseki, T. Onodera, H. Oikawa, H. Kasai, Creation of nano eye-drops and effective drug delivery to the interior of the eye, Sci. Rep. 7 (2017) 44229, https://doi.org/10.1038/srep44229.

[12] D.R. Janagam, L. Wu, T.L. Lowe, Nanoparticles for drug delivery to the anterior segment of the eye, Adv. Drug Deliv. Rev. 122 (2017) 31–64, https://doi.org/10.1016/j.addr.2017.04.001.

[13] H.S.B. Sai, Polymeric nanoparticles for ophthalmic drug delivery: an update on research and patenting activity, Recent Pat. Nanomed. 2 (2012) 96–112, https://doi.org/10.2174/1877912311202020096.

[14] E. Sánchez-López, M.A. Egea, B.M. Davis, L. Guo, M. Espina, A.M. Silva, A. C. Calpena, E.M.B. Souto, N. Ravindran, M. Ettcheto, A. Camins, M.L. García, M. F. Cordeiro, Memantine-loaded PEGylated biodegradable nanoparticles for the treatment of glaucoma, Small 14 (2018) 1701808, https://doi.org/10.1002/smll.201701808.

[15] L.J. Luo, D.D. Nguyen, J.Y. Lai, Dually functional hollow ceria nanoparticle platform for intraocular drug delivery: a push beyond the limits of static and dynamic ocular barriers toward glaucoma therapy, Biomaterials 243 (2020) 16, https://doi.org/10.1016/j.biomaterials.2020.119961.

[16] C. Hu, J. Sun, Y. Zhang, J. Chen, Y. Lei, X. Sun, Y. Deng, Local delivery and sustained-release of nitric oxide donor loaded in mesoporous silica particles for efficient treatment of primary open-angle glaucoma, Adv. Healthc. Mater. 7 (2018) 1801047, https://doi.org/10.1002/adhm.201801047.

[17] S. Swetledge, J.P. Jung, R. Carter, C. Sabliov, Distribution of polymeric nanoparticles in the eye: implications in ocular disease therapy, J. Nanobiotechnol. 19 (2021) 10, https://doi.org/10.1186/s12951-020-00745-9.

[18] S.-N. Kim, S.A. Ko, C.G. Park, S.H. Lee, B.K. Huh, Y.H. Park, Y.K. Kim, A. Ha, K. H. Park, Y.B. Choy, Amino-functionalized mesoporous silica particles for ocular delivery of brimonidine, Mol. Pharm. 15 (2018) 3143–3152, https://doi.org/10.1021/acs.molpharmaceut.8b00215.

[19] J. Wang, H. He, R.C. Cooper, H. Yang, In situ-forming polyamidoamine dendrimer hydrogels with tunable properties prepared via aza-Michael addition reaction, ACS Appl. Mater. Interfaces 9 (2017) 10494–10503, https://doi.org/10.1021/acsami.7b00221.

[20] J. Wang, G.S. Williamson, M.G. Lancina III, H. Yang, Mildly cross-linked dendrimer hydrogel prepared via aza-Michael addition reaction for topical brimonidine delivery, J. Biomed. Nanotechnol. 13 (2017) 1089–1096, https://doi.org/10.1166/jbn.2017.2436.

[21] M.G. Lancina III, H. Yang, Dendrimers for ocular drug delivery, Can. J. Chem. 95 (2017) 897–902, https://doi.org/10.1139/cjc-2017-0193.

[22] S. Kannan, H. Dai, R.S. Navath, B. Balakrishnan, A. Jyoti, J. Janisse, R. Romero, R. M. Kannan, Dendrimer-based postnatal therapy for neuroinflammation and cerebral palsy in a rabbit model, Sci. Transl. Med. 4 (2012) 130ra46, https://doi.org/10.1126/scitranslmed.3003162.

[23] D.A. Tomalia, L.S. Nixon, D.M. Hedstrand, The role of branch cell symmetry and other critical nanoscale design parameters in the determination of dendrimer encapsulation properties, Biomolecules 10 (2020) 642, https://doi.org/10.3390/biom10040642.

[24] J. Wang, R.C. Cooper, H. He, B. Li, H. Yang, Polyamidoamine dendrimer microgels: Hierarchical arrangement of dendrimers into micrometer domains with expanded structural features for programmable drug delivery and release, Macromolecules 51 (2018) 6111–6118, https://doi.org/10.1021/acs.macromol.8b01006.

[25] J.C. Cuggino, L.I. Tartara, L.M. Gugliotta, S.D. Palma, C.I. Alvarez Igarzabal, Mucoadhesive and responsive nanogels as carriers for sustainable delivery of timolol for glaucoma therapy, Mat. Sci. Eng. C 118 (2021), https://doi.org/10.1016/j.msec.2020.111383.

[26] L. Serra, J. Doménech, N.A. Peppas, Drug transport mechanisms and release kinetics from molecularly designed poly(acrylic acid-g-ethylene glycol) hydrogels, Biomaterials 27 (2006) 5440–5451, https://doi.org/10.1016/j.biomaterials.2006.06.011.

[27] Q. Yuan, Y. Fu, W.J. Kao, D. Janigro, H. Yang, Transbuccal delivery of CNS therapeutic nanoparticles: synthesis, characterization, and in vitro permeation studies, ACS Chem. Neurosci. 2 (2011) 676–683, https://doi.org/10.1021/cn200078m.

[28] L. Xu, N. Sheybani, S. Ren, G.L. Bowlin, W.A. Yeudall, H. Yang, Semi-interpenetrating network (sIPN) co-electrospun gelatin/insulin fiber formulation for transbuccal insulin delivery, Pharm. Res. 32 (2015) 275–285, https://doi.org/10.1007/s11095-014-1461-9.

[29] L. Xu, O.Y. Zolotarskaya, W.A. Yeudall, H. Yang, Click hybridization of immune cells and polyamidoamine dendrimers, Adv. Healthc. Mater. 3 (2014) 1430–1438, https://doi.org/10.1002/adhm.201300515.

[30] M.H. Asim, M. Ijaz, A. Mahmood, P. Knoll, A. Jalil, S. Arshad, A. Bernkop-Schnürch, Thiolated cyclodextrins: mucoadhesive and permeation enhancing excipients for ocular drug delivery, Int. J. Pharm. 599 (2021), 120451, https://doi.org/10.1016/j.ijpharm.2021.120451.

[31] B.R. Thomson, M. Grannonico, F. Liu, M. Liu, P. Mendapara, Y. Xu, X. Liu, S. E. Quaggin, Angiopoietin-1 knockout mice as a genetic model of open-angle glaucoma, Transl. Vis. Sci. Technol. 9 (2020) 16, https://doi.org/10.1167/tvst.9.4.16.

[32] I. Durocher, D. Girard, In vivo proinflammatory activity of generations 0–3 (G0–G3) polyamidoamine (PAMAM) nanoparticles, Inflamm. Res. 65 (2016) 745–755, https://doi.org/10.1007/s00011-016-0959-5.

[33] P.C. Naha, M. Davoren, F.M. Lyng, H.J. Byrne, Reactive oxygen species (ROS) induced cytokine production and cytotoxicity of PAMAM dendrimers in J774A.1 cells, Toxicol. Appl. Pharm. 246 (2010) 91–99, https://doi.org/10.1016/j.taap.2010.04.014.

[34] J.M. Martinez-de-la-Casa, F. Perez-Bartolome, E. Urcelay, J.L. Santiago, J. Moreno-Montañes, P. Arriola-Villalobos, J.M. Benitez-del-Castillo, J. Garcia-Feijoo, Tear cytokine profile of glaucoma patients treated with preservative-free or preserved latanoprost, Ocul. Surf. 15 (2017) 723–729, https://doi.org/10.1016/j.jtos.2017.03.004.

[35] C. Solans, P. Izquierdo, J. Nolla, N. Azemar, M.J. Garcia-Celma, Nano-emulsions, Curr. Opin. Colloid Interface Sci. 10 (2005) 102–110, https://doi.org/10.1016/j.cocis.2005.06.004.

[36] T.F. Tadros, Emulsion formation, stability, and rheology, in: T.F. Tadros (Ed.), Emulsion Formation and Stability, Wiley-VCH Verlag GmbH & Co. KGaA, 2013, pp. 1–75.

[37] J. Wang, H. He, R.C. Cooper, Q. Gui, H. Yang, Drug-conjugated dendrimer hydrogel enables sustained drug release via a self-cleaving mechanism, Mol. Pharm. 16 (2019) 1874–1880, https://doi.org/10.1021/acs.molpharmaceut.8b01207.

[38] T. Souma, S.W. Tompson, B.R. Thomson, O.M. Siggs, K. Kizhatil, S. Yamaguchi, L. Feng, V. Limviphuvadh, K.N. Whisenhunt, S. Maurer-Stroh, T.L. Yanovitch, L. Kalaydjieva, D.N. Azmanov, S. Finzi, L. Mauri, S. Javadiyan, E. Souzeau, T. Zhou, A.W. Hewitt, B. Kloss, K.P. Burdon, D.A. Mackey, K.F. Allen, J.B. Ruddle, S.H. Lim, S. Rozen, K.N. Tran-Viet, X. Liu, S. John, J.L. Wiggs, F. Pasutto, J. E. Craig, J. Jin, S.E. Quaggin, T.L. Young, Angiopoietin receptor TEK mutations underlie primary congenital glaucoma with variable expressivity, J. Clin. Invest. 126 (2016) 2575–2587, https://doi.org/10.1172/JCI85830.

[39] B.R. Thomson, S. Heinen, M. Jeansson, A.K. Ghosh, A. Fatima, H.K. Sung, T. Onay, H. Chen, S. Yamaguchi, A.N. Economides, A. Flenniken, N.W. Gale, Y.K. Hong, A. Fawzi, X. Liu, T. Kume, S.E. Quaggin, A lymphatic defect causes ocular hypertension and glaucoma in mice, J. Clin. Invest. 124 (2014) 4320–4324, https://doi.org/10.1172/JCI77162.

[40] B.R. Thomson, T. Souma, S.W. Tompson, T. Onay, K. Kizhatil, O.M. Siggs, L. Feng, K.N. Whisenhunt, T.L. Yanovitch, L. Kalaydjieva, D.N. Azmanov, S. Finzi, C. E. Tanna, A.W. Hewitt, D.A. Mackey, Y.S. Bradfield, E. Souzeau, S. Javadiyan, J. L. Wiggs, F. Pasutto, X. Liu, S.W. John, J.E. Craig, J. Jin, T.L. Young, S.E. Quaggin, Angiopoietin-1 is required for Schlemm's canal development in mice and humans, J. Clin. Invest. 127 (2017) 4421–4436, https://doi.org/10.1172/JCI95545.